

Effects of electric microfields on argon dielectronic satellite spectra in laser-produced plasmas

L. A. Woltz*

Atomic and Plasma Radiation Division, National Institute of Standards and Technology, Gaithersburg, Maryland 20899

V. L. Jacobs

Condensed Matter and Radiation Sciences Division (Code 4694), Naval Research Laboratory, Washington, D.C. 20375-5000

C. F. Hooper, Jr. and R. C. Mancini

Department of Physics, University of Florida, Gainesville, Florida 32611

(Received 3 April 1990; revised manuscript received 27 December 1990)

Theoretical spectral-line profiles have been obtained for dielectronic satellite transitions in heliumlike and lithiumlike argon ions. Particular emphasis has been given to the systematic and self-consistent incorporation of the non-local-thermodynamic-equilibrium autoionizing-level populations, together with the line-broadening effects, which are due to autoionization processes, radiative transitions, electron collisions, and the action of the plasma ion-produced electric microfields. An investigation has been carried out of the effects of the plasma electric microfields on predicted dielectronic satellite line-intensity ratios, and a discussion is presented on the consequences of the electric-microfield effects for the spectroscopic determination of basic physical properties in laser-produced plasmas.

I. INTRODUCTION

The analysis of the dielectronic satellite lines emitted from autoionizing states of atomic ions has proved to be useful for the spectroscopic determination of the temperature and density of laser-produced plasmas. Both satellite-to-resonance-line and relative satellite-line intensity ratios have been employed in this analysis. The spectral-line intensities and line-profile functions which are required for the prediction of these intensity ratios are determined by the combined actions of a multitude of elementary atomic collision and radiation processes, and the rates and line-profile parameters describing these processes are in turn dependent on the temperature and density in the plasma.

Considerable effort has been expended in the development of the theoretical basis for the prediction of these spectral-line intensities and line-profile functions. Elementary atomic processes such as electron collisional transitions, spontaneous radiative emissions, and autoionization processes have been taken into account in detailed theoretical treatments.¹ Recently, Bañón and co-workers have investigated the broadening of dielectronic satellite lines by the action of the plasma electric microfields, employing two-state eigenvalue calculations of ion-microfield-induced energy-level shifts but assuming local-thermodynamic-equilibrium (LTE) autoionizing-level populations.²⁻⁴ These results clearly show the importance of field-mixing effects among certain doubly excited states.

The primary objective of the present investigation has been the systematic determination of the spectral-line intensities and line profile functions for dielectronic satellite transitions by self-consistently taking into account, in

both the determination of the non-LTE level populations and the description of the line broadening, the same set of elementary atomic autoionization, radiative decay, and electron collision processes, together with the effects of the plasma ion-produced electric microfields. Results of our calculations will be presented for dielectronic satellite transitions in heliumlike and lithiumlike argon ions. In each case all the relevant $2l2l'$ and $1s2l2l'$ doubly excited states together with the $1s2l$ and $1s^22l$ singly excited states have been included in our calculation. These transitions give rise to prominent spectroscopic features in laser-produced plasmas, which have been extensively used for determinations of basic plasma properties.

II. DESCRIPTION OF THE SPECTRAL-LINE-PROFILE CALCULATION

Using the static-ion approximation in the general overlapping-line-shape theory, the spectral-line-profile function may be expressed in the form⁵

$$I(\omega) = \int_0^\infty P(\epsilon) J(\omega, \epsilon) d\epsilon, \quad (1)$$

where $P(\epsilon)$ denotes the static-ion-produced electric-microfield probability distribution function⁶ and $J(\omega, \epsilon)$ is the electron-collision-broadened line-profile function evaluated for the particular value ϵ of the ion-produced electric microfield. The electron-collision-broadened line-profile function may be presented, using Liouville-space notation, in the form⁵

$$J(\omega, \epsilon) = -\frac{1}{\pi} \text{Im} \sum_{i, j, i', j'} \rho_i \mathbf{d}_{f' i'} [\omega - L_R(\epsilon) - M(\omega)]_{i' f', i f}^{-1} \mathbf{d}_{i f}. \quad (2)$$

Here, i and f represent, respectively, the initial and final states of the atomic system undergoing the radiative transition (the radiator), ρ is the density operator representing the population distribution among the initial atomic levels, which is assumed to have only diagonal matrix elements ρ_i , d is the radiator dipole-moment operator, $M(\omega)$ is the tetradic frequency-dependent electron collisional broadening operator, and $L_R(\epsilon)$ is the radiator Liouville-space operator. $L_R(\epsilon)$ can be defined as the commutator

$$L_R(\epsilon) \equiv [H_R(\epsilon), \rho] \quad (3)$$

where $H_R(\epsilon)$ is the Hamiltonian for the radiating atomic system in the presence of the ion-produced electric field ϵ .

The electron collisional broadening operator $M(\omega)$ has been evaluated to second order in the radiator-electron interaction, which is taken to be the long-range dipole interaction. The evaluation of $M(\omega)$ involves an average over the perturbing electron states, which are represented in this investigation by Coulomb wave functions. The form of the electron collisional broadening operator is discussed further in Refs. 7 and 8.

The formalism described above has provided the basis for a multielectron ion spectral-line broadening code,⁸ which has been employed for the calculation of the resonance-line profiles broadened by the plasma-electron collisions and the action of the plasma ion-produced electric microfields. In the present investigation for dielectronic satellite transitions, this code has been extended to incorporate the additional broadening due to radiative transitions and autoionization processes and to utilize non-LTE autoionizing-level populations.

The input data set that is required for the operation of the spectral-line-broadening code includes the unperturbed energy-level eigenvalues and the reduced matrix elements of the dipole-moment operator for the transitions of interest. The required data set has been obtained from the relativistic multiconfiguration atomic structure codes of Cowan.⁹ The plasma ion-produced electric-microfield distribution must also be supplied. This distribution has been calculated using the electric-microfield codes of Tighe and Hooper.⁶ The peaks of the microfield distributions used in this work are at 1.74×10^{10} , 8.07×10^{10} , and 3.74×10^{11} V m⁻¹ for electron densities of 10^{22} , 10^{23} , and 10^{24} cm⁻³. In the present calculation, the spectral-line-broadening profile function has been evaluated using an unperturbed atomic basis set. Consequently, the effects of the ion-produced electric microfield are described by off-diagonal matrix elements of the radiator Hamiltonian $H_R(\epsilon)$, as is discussed in Ref. 8.

The broadening due to the combined mechanisms of autoionization, radiative decay, and electron collisions, to a first approximation, can be described by the sum of the widths that each individual mechanism would produce when acting alone.¹ The spectral-line-broadening code generates the tetradic matrix $M(\omega)$, which represents the electron collisional broadening.⁸ To take into account the additional broadening due to autoionization and radiative decay processes, we have augmented the diagonal elements of this tetradic matrix to include the corre-

sponding spontaneous widths, which are independent of the electric field. The field-induced mixing of the autoionizing states, which is described by the matrix inversion in Eq. (2), results in field-dependent widths. When the Stark splitting of the autoionizing levels is small in comparison with their separation, the widths are predicted, using the quadratic-Stark-effect approximation, to be proportional to ϵ^2 . When the Stark splitting is comparable to the level separation, the field dependence of the width becomes much weaker. To incorporate non-LTE plasma effects, the matrix elements of the density operator ρ have been determined by employing the non-LTE autoionizing-level population densities that have been obtained using the atomic physics model described in Ref. 1. The effects of interference between autoionization and radiative decay were investigated using the same model, and were found to be small for the plasma conditions of this work. The influence of the ion-produced electric microfields on the populations of the autoionizing levels and the explicit field dependence of their linewidths will be investigated in an extension of the present calculation, which will be presented in a separate publication.

III. DIELECTRONIC SATELLITE TRANSITIONS IN HELIUMLIKE AND LITHIUMLIKE ARGON

In this section we present our theoretical results for the profiles of the dielectronic satellite lines of heliumlike and lithiumlike argon. We have investigated the relative importance of the broadening due to electron collisions (EC), radiative decay (RD), autoionization (AI), and the Doppler effect. We present comparisons of satellite-line profiles calculated with and without the ion-produced electric-microfield effects, and we show comparisons of the satellite-line profile calculated using LTE and non-LTE populations for the autoionizing levels. We have considered electron densities from 10^{22} to 10^{24} cm⁻³; this approximately covers the density range between the regions of validity of the coronal and LTE models for the atomic level populations.

In Fig. 1, we show comparisons of the He-like Ar

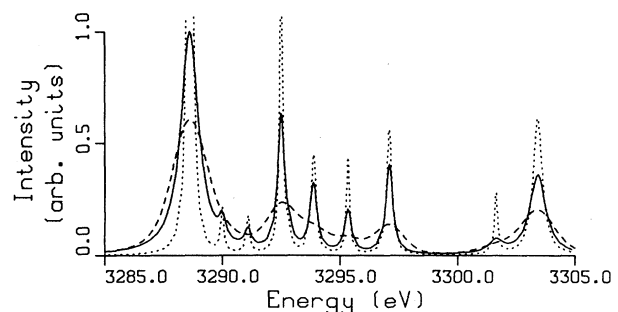


FIG. 1. Heliumlike argon $1s2l-2l2l'$ satellite-line profiles broadened by electron collisions (dotted curve), by electron collisions, radiative decay, and autoionization (solid curve), by electron collisions, radiative decay, autoionization, and the Doppler effect (dashed curve). Temperature, 1000 eV; electron density, 10^{23} cm⁻³.

$1s2l-2l2l'$ satellite-line profiles broadened only by EC (dotted curve), by EC, RD, and AI (solid curve), and by EC, RD, AI, and the Doppler effect (dashed curve). These profiles do not include ion microfield effects and have been calculated for a temperature of 1000 eV and an electron density of 10^{23} cm^{-3} . Non-LTE autoionizing-level populations were utilized in this calculation. At this density, the EC broadening is about as effective as the broadening due to RD and AI. At 10^{22} cm^{-3} the EC broadening, which is proportional to the electron density, is expected to be negligible in comparison with the RD and AI broadening. At 10^{24} cm^{-3} the EC broadening is predicted to be dominant over the RD and AI broadening. In the density range from 10^{22} to 10^{23} cm^{-3} , the Doppler broadening is found to be dominant over the EC, RD, and AI broadening. At a density of 10^{24} cm^{-3} , however, the EC broadening exceeds the Doppler broadening.

Figure 2 shows a comparison of He-like Ar satellite-line profiles calculated with (solid curve) and without (dashed curve) the inclusion of the broadening resulting from the action of the ion-produced electric microfields. The line profiles presented in this figure (as well as those shown in Figs. 3–6) include the EC, RD, AI, and Doppler broadening. As indicated, these line profiles were calculated for electron densities of 10^{22} , 10^{23} , and 10^{24} cm^{-3} and for a temperature of 1000 eV. Non-LTE autoionizing-level populations were utilized for these calculations. The peak at 3289 eV is associated with the $1s2p^1P-2p^2^1D$ transition. The peaks between 3290 and 3300 eV correspond to the $1s2p^3P-2p^2^3P$ and $1s2s^3S-2s2p^3P$ transitions. The peak at 3303.4 eV arises from the $1s2s^1S-2s2p^1P$ transition. The $2s2p^1P$ and $2p^2^1D$ autoionizing levels are very close to each other in energy (0.9 eV) and are strongly mixed by the action of the ion-produced electric microfields. This mixing gives rise to forbidden transitions, which can be seen near 3286 and 3306 eV. In Refs. 10 and 11, a numerical fitting of Lorentzian profile functions to experimental He-like Ar satellite-line profiles was performed to determine the ratios of the individual component intensities. The fitting program employed in these references consistently predicted a Lorentzian line profile located to the left of the $1s2p^1P-2p^2^1D$ transition. The line profiles calculated in the present investigation indicate that this peak, which was not identified in Refs. 10 and 11, is associated with the forbidden transition $1s2p^1P-2s2p^1P$. The relatively small separation of the $2s2p^1P$ and $2p^2^1D$ autoionizing levels also causes them to exhibit large Stark shifts, and hence a relatively large ion-produced electric-microfield broadening, in comparison with that of the triplet transitions. Ion-produced electric-microfield broadening begins to be significant for the singlet transitions at a density of only 10^{22} cm^{-3} , and it becomes the predominant broadening mechanism for higher densities. He-like Ar satellite-line profiles calculated at the same densities and at a lower temperature of 600 eV were found to be slightly narrower than for the 1000-eV case. The overall line shapes were found to be almost the same as those obtained at the higher 1000-eV temperature, reflecting the temperature insensitivity of the relative populations for

the He-like Ar autoionizing levels over this particular temperature range. The intensity ratios of various components of the He-like Ar satellite lines have been extensively investigated in connection with the spectroscopic determination of plasma densities and temperatures,^{1,10,11} but ion-produced electric-microfield effects were not taken into account in those investigations.

Figure 2 shows that the ion-produced electric microfields can have significant effects on the individual line intensity ratios that involve the singlet transitions. The electric-microfield-induced mixing of radiator states is found to result in a transfer of line intensity from each

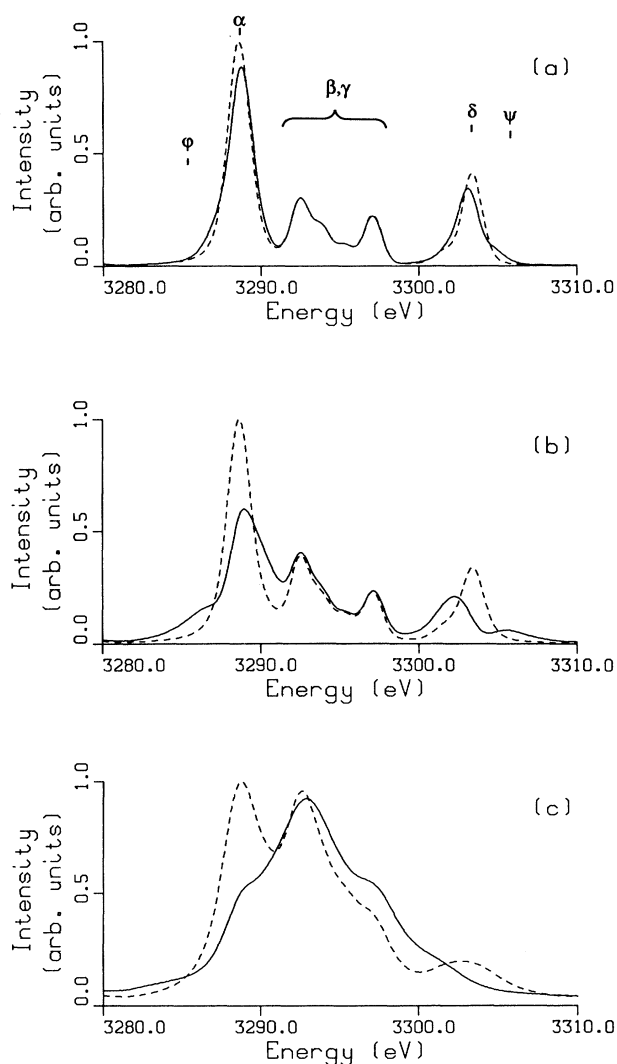


FIG. 2. Heliumlike argon $1s2l-2l'$ satellite-line profiles, including (solid curve) and neglecting (dashed curve) the effects of the ion-produced electric microfields. Temperature, 1000 eV; electron density: (a) 10^{22} , (b) 10^{23} , and (c) 10^{24} cm^{-3} . The transitions which contribute to these profiles are (α) $1s2p^1P-2p^2^1D$, (β) $1s2p^3P-2p^2^3P$, (γ) $1s2s^3S-2s2p^3P$, (δ) $1s2s^1S-2s2p^1P$, (ϕ) and (ψ) forbidden transitions arising from field-induced mixing of $2s2p^1P$ and $2p^2^1D$.

allowed transition to forbidden transitions having the same final atomic level. The total intensity of allowed plus forbidden transitions involving these $n=2$ levels is found to be little affected by the presence of the electric microfields. We note that in the current version of our calculation, the influence of the ion-produced electric microfields on the autoionizing-level populations has not been taken into account and the unperturbed widths are independent of the field.

In this connection, the electron-density-sensitive intensity ratio of the triplet transitions $1s2p^3P-2p^2^3P$ and $1s2s^3S-2s2p^3P$ with respect to the singlet $1s2p^1P-2p^2^1P$ is expected to increase in comparison with the value obtained using field-independent spectral-line analysis. For example, we have estimated that for an electron density of 10^{23} cm^{-3} , inclusion of ion microfield effects changes this ratio from 0.66 to 0.82. The ratio of 0.82 corresponds to a density of $2 \times 10^{23} \text{ cm}^{-3}$ in a field-independent analysis. Consequently, an electron-density

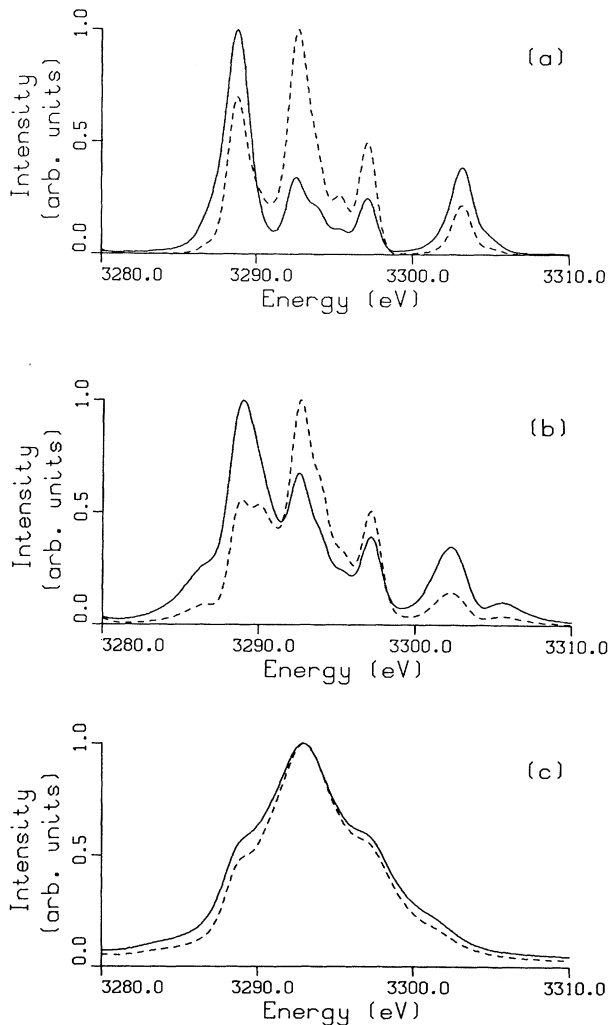


FIG. 3. Heliumlike argon $1s2l-2l'$ satellite-line profiles calculated utilizing LTE (dashed curve) and non-LTE (solid curve) autoionizing-level populations. Temperature, 1000 eV; electron density: (a) 10^{22} , (b) 10^{23} , and (c) 10^{24} cm^{-3} .

determination based on this ratio but neglecting field-mixing effects will tend to overestimate the electron density. This is consistent with the trend observed in Ref. 10, where electron densities determined from triplet-to-singlet satellite intensity ratios (neglecting ion microfields) were significantly greater than densities determined by resonance linewidth analysis.

For an accurate determination of the basic plasma properties from the analysis of experimental dielectronic satellite-line spectra, all effects of the ion-produced electric microfields should be self-consistently taken into account in the prediction of the satellite-line profiles. The fitting of experimental spectra by the use of simple Lorentzian or Voigt line-profile functions is complicated by the large differences among the Lorentzian widths predicted for the individual peaks, the significant overlap of peaks for electron densities above 10^{22} cm^{-3} , and the asymmetric broadening due to the action of the ion-produced electric microfields. The fitting of full theoretical satellite-line profiles to the corresponding experimentally observed line profiles would be expected to circumvent these difficulties.

Figure 3 shows the difference between He-like Ar satellite-line profiles obtained with the utilization of LTE and non-LTE autoionizing-level populations. These line profiles were calculated for a temperature of 1000 eV and for electron densities of 10^{22} , 10^{23} , and 10^{24} cm^{-3} . The non-LTE populations of the autoionizing levels differ substantially from those obtained in the LTE approximation at 10^{22} cm^{-3} , but are close to the LTE populations at 10^{24} cm^{-3} .

The non-LTE populations of the Li-like autoionizing levels are found to be especially sensitive to temperature for electron densities below 10^{24} cm^{-3} . This can be seen in Fig. 4, in which we compare Li-like Ar satellite-line profiles calculated for temperatures of 600 and 1000 eV and for an electron density of 10^{22} cm^{-3} . These transi-

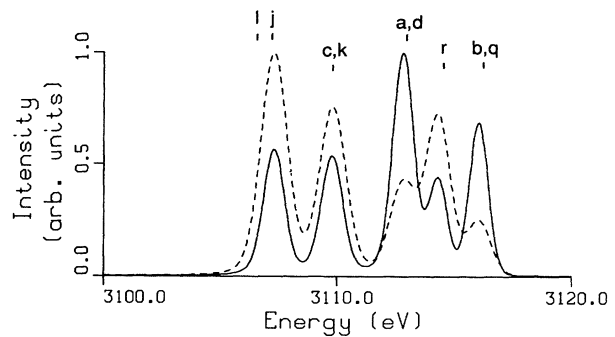


FIG. 4. Lithiumlike argon $1s^2l-1s^2l'$ satellite-line profiles calculated at 600 eV (solid curve) and 1000 eV (dashed curve). Electron density, 10^{22} cm^{-3} . The transitions are (l) $1s2p^2^2D_{3/2}-1s^22p^2P_{3/2}$, (j) $1s2p^2^2D_{5/2}-1s^22p^2P_{3/2}$, (c) $1s2p^2^2P_{1/2}-1s^22p^2P_{3/2}$, (k) $1s2p^2^2D_{3/2}-1s^22p^2P_{1/2}$, (a) $1s2p^2^2P_{3/2}-1s^22p^2P_{3/2}$, (d) $1s2p^2^2P_{1/2}-1s^22p^2P_{1/2}$, (r) $1s2s(^1S_0)2p^2P_{1/2}-1s^22s^2S_{1/2}$, (b) $1s2p^2^2P_{3/2}-1s^22p^2P_{1/2}$, and (q) $1s2s(^1S_0)2p^2P_{3/2}-1s^22s^2S_{1/2}$. The letter designations for the transitions are the same as those used in Ref. 1.

tions are of the type $1s^22l-1s2l2l'$.

The Li-like satellite-line profiles are found to be much less sensitive to the effects of the ion-produced electric microfields than are the He-like satellite-line profiles. We note that the energy-level separations of the initial Li-like autoionizing states are larger than for the He-like singlet states. Consequently, the field-induced mixing of unperturbed Li-like autoionizing states and the resulting energy-level shifts are smaller. However, at a density of 10^{24} cm^{-3} , the ion-produced electric microfields begin to have a significant effect on the Li-like satellite-line profile, as can be seen in Fig. 5.

In Fig. 6 we compare Li-like Ar satellite-line profiles calculated with the utilization of LTE and non-LTE autoionizing-level populations. As in the He-like case, the satellite-line profiles are found to differ substantially at 10^{22} cm^{-3} and to approach each other at 10^{24} cm^{-3} .

The static-ion approximation will be valid for these spectral lines if the mean lifetime of the radiator initial state is small compared to the time scale for radiator-perturber relative motion, or if the parameter⁵ $\sigma = \omega_e \rho_m / \nu_r$ is greater than one. Here, ω_e is the line half-width at half maximum due to EC, RD, and AI, ρ_m is the mean interion distance, and ν_r is the mean radiator-ion relative velocity. At electron densities of 10^{22} , 10^{23} , and 10^{24} cm^{-3} , the $1s2p^1P-2p^2^1D$ transition has σ values of 3.4, 1.9, and 3.3, so that the static-ion approximation will be valid. Although some of the He-like triplet transitions and the Li-like transitions have σ values close to or slightly below one for the lower densities, any ion-dynamic effects in these lines should be nearly negligible when Doppler broadening is added to the spectra.

IV. CONCLUSIONS

We have investigated the plasma broadening of He-like and Li-like Ar dielectronic satellite-line profiles, with particular emphasis on the relative importance of the broadening due to autoionization and radiative decay, electron collisional broadening, ion-produced electric-microfield broadening, and Doppler broadening. We

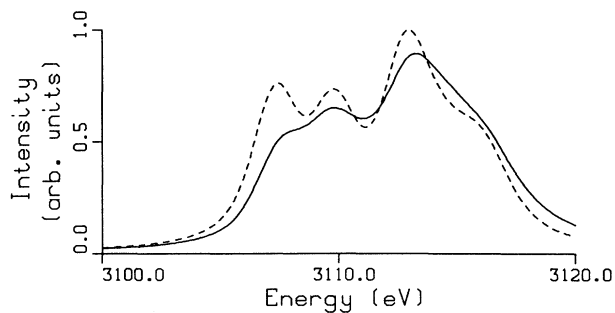


FIG. 5. Lithiumlike argon $1s^22l-1s2l2l'$ satellite-line profiles obtained including (solid curve) and neglecting (dashed curve) the effects of the ion-produced electric microfields. Temperature, 1000 eV; electron density, 10^{24} cm^{-3} .

have demonstrated that the plasma ion-produced electric microfields have a significant effect on He-like Ar dielectronic satellite line-intensity ratios. The ion-produced electric microfields affect the Li-like Ar satellite lines to a lesser degree, but the microfield effects can become significant at the highest densities considered in this investigation. The relative populations of the Li-like autoionizing levels are found to be particularly sensitive to temperature, giving rise to a corresponding temperature sensitivity in the predicted Li-like satellite-line profiles. The He-like Ar satellite-line profiles show much less temperature sensitivity.

In a future extension of this investigation, we plan to

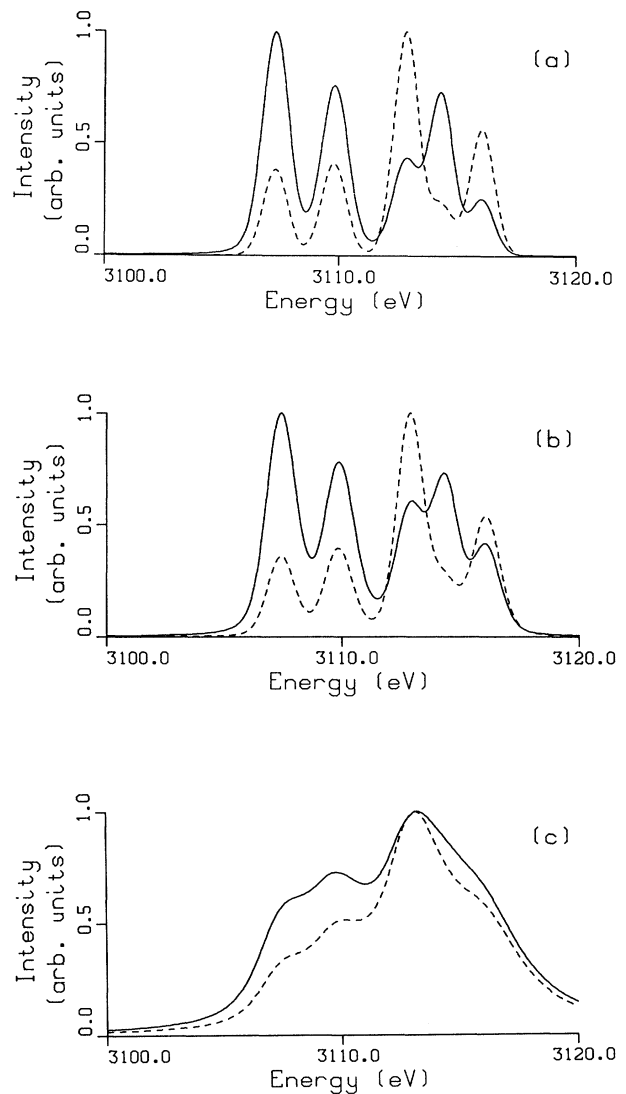


FIG. 6. Lithiumlike argon $1s^22l-1s2l2l'$ satellite-line profiles calculated incorporating LTE (dashed curve) and non-LTE (solid curve) autoionizing-level populations. Temperature, 1000 eV; electron density: (a) 10^{22} , (b) 10^{23} , and (c) 10^{24} cm^{-3} .

incorporate a calculation that will provide the autoionizing-level population densities and linewidths as functions of the ion-produced electric field. This extension will allow a direct investigation of the field-induced radiationless electron-capture process, which has been predicted to play an increasingly important role for the more highly excited autoionizing levels belonging to the electronic configurations $2lnl'$ and $1s2lnl'$ with $n > 3$.¹²

ACKNOWLEDGMENTS

The authors wish to thank Dr. J. F. Seely for helpful discussions. This investigation has been supported by the National Laser Users Facility of the University of Rochester Laboratory for Laser Energetics, by the Lawrence Livermore National Laboratory, and by the U.S. Department of Energy.

*Present address: American Electronics, Inc., 9332 Annapolis Road, Lanham, MD 20706.

¹V. L. Jacobs, J. E. Rogerson, M. H. Chen, and R. D. Cowan, *Phys. Rev. A* **32**, 3382 (1985).

²J. M. Bañón, L. L. Sanchez-Soto, and E. Bernabeu, *J. Phys. B* **22**, 199 (1989).

³J. M. Bañón, and H. Nguyen, *J. Phys. B* **20**, 2989 (1987).

⁴J. M. Bañón, M. Koenig, and H. Nguyen, *J. Phys. B* **18**, 4195 (1985).

⁵H. R. Griem, *Spectral Line Broadening by Plasmas* (Academic, New York, 1974).

⁶C. F. Hooper, Jr., *Phys. Rev.* **165**, 215 (1968); Richard J. Tighe and C. F. Hooper, Jr., *Phys. Rev. A* **15**, 1773 (1977).

⁷John T. O'Brien and C. F. Hooper, Jr., *J. Quant. Spectrosc.*

Radiat. Transfer **14**, 479 (1974).

⁸L. A. Woltz and C. F. Hooper, Jr., *Phys. Rev. A* **38**, 4766 (1988).

⁹Robert D. Cowan, *The Theory of Atomic Structure and Spectra* (University of California Press, Berkeley, 1981).

¹⁰N. D. Delamater *et al.*, in *Radiative Properties of Hot Dense Matter*, edited by Jack Davis, Charles Hooper, Richard Lee, Allen Merts, and Balazs Rozsnyai (World Scientific, Singapore, 1985).

¹¹N. D. Delamater, Ph.D. dissertation, University of Florida, Gainesville, 1984.

¹²V. L. Jacobs, in *Atomic Excitation and Recombination in External Fields*, edited by M. H. Nayfeh and C. W. Clark (Gordon and Breach, London, 1985).